J Therm Anal Calorim (2010) 102:875–881
DOI 10.1007/s10973-010-0702-3

Re-investigations of thermal decomposition of gadolinium sulfate octahydrate

E. Tomaszewicz · G. Leniec · S. M. Kaczmarek

Received: 12 January 2010 / Accepted: 27 January 2010 / Published online: 18 February 2010

Abstract The crystals of $Gd_2(SO_4)_3 \cdot 8H_2O$ were obtained by slow crystallization from a saturated solution previously received by dissolving Gd_2O_3 in an aqueous solution of sulfuric acid. The thermal behavior of this salt was studied using simultaneous DTA–TG technique under a nitrogen and air, in the temperature range of 298–1773 K. It was found that the dehydration of gadolinium sulfate octahydrate as well as thermal decomposition of anhydrous $Gd_2(SO_4)_3$ undergo in two steps. The existence of two polymorphic modification of anhydrous gadolinium sulfate has been confirmed. The new XRD data for high-temperature polymorph of $Gd_2(SO_4)_3$ were given. All intermediate products of dehydration and thermal decomposition were characterized by EPR method.

Keywords Gadolinium sulfate octahydrate · Thermal decomposition · IR · EPR

Introduction

Thermal dehydration and decomposition studies of metal salts hydrates have gained significant importance [1, 2]. One of the reasons is the ability to receive, in these processes, materials with high-grade purity. Rare-earth metal salts are used to receiving many materials that are relevant from a technological point of view (superconducting and electronic materials, high efficiency phosphors, rare-earth magnets, catalysts, and pigments) [3–9]. Lanthanides form a series of compounds with properties that change regularly with increasing atomic number of lanthanide. Among many oxysalts, the sulfates hydrates are easily obtained as well-grown crystals from aqueous solutions. Most of the salts are octahydrates with the monoclinic structure.

Gadolinium sulfate octahydrate crystallizes in the monoclinic system with the space group *C2/c* and the lattice constants: $a = 1.3531(7)$, $b = 0.6739(2)$, $c = 1.8294(7)$ nm, $\beta = 102.20(8)°$ [10]. In the structure of this compound, Gd^{3+} ions are coordinated by 4 oxygen ions of the crystal water and 4 oxygen ions from the sulfate groups giving rise to a distorted square antyprisms [10]. The luminescence of Pr^{3+}-doped gadolinium sulfate hydrates and both polymorphic modifications of anhydrous $Gd_2(SO_4)_3$ was reported under 195 nm laser excitation [11]. The Pr^{3+} ions were used as a sensitizer of the host lattice emission. It was found that the $Pr^{3+} \rightarrow Gd^{3+}$ energy transfer was, in the case of octahydrate, hydrate with less crystal water as well as both polymorphs of anhydrous $Gd_2(SO_4)_3$, different [11].

In the present article, we report the synthesis, thermal dehydration of $Gd_2(SO_4)_3 \cdot 8H_2O$ and decomposition of anhydrous $Gd_2(SO_4)_3$. The intermediate solid products and final product of decomposition were analyzed by XRD, IR, and EPR techniques.

Experimental

Preparation of gadolinium sulfate octahydrate

Gadolinium oxide (Gd_2O_3, 99.9%, Aldrich) was dissolved, during heating, in a diluted sulfuric acid. After complete dissolution, the solution was concentrated slowly by

E. Tomaszewicz (✉)
Department of Inorganic and Analytical Chemistry,
West Pomeranian University of Technology, Al.Piastów 42,
71-065 Szczecin, Poland
e-mail: tomela@zut.edu.pl

G. Leniec · S. M. Kaczmarek
Institute of Physics, West Pomeranian University of Technology,
Al.Piastów 17, 70-310 Szczecin, Poland

evaporation at 333 K. Crystalline gadolinium sulfate hydrate formed in the concentrate was filtered with sintered glass crucible and washed with small amount of double-distilled water and then acetone. The obtained crystals were finally dried in air and stored in a desiccator.

Characterization of used methods

The X-ray powder data were recorded on a DRON-3 diffractometer employing Co Kα radiation ($\lambda = 0.179021$ nm). Powder diffraction patterns were collected in the 2θ range of 12°–52° at the stepped scan rate of 0.02° per step and the count time of 1 s per step.

DTA–TG examinations were performed using a Mettler Toledo TGA/SDTA851 thermoanalyzer. The experiments were carried out within the temperature range of 298–1773 K, in air and a nitrogen atmosphere, using corundum crucibles and the heating rate of 10 K min^{-1}.

The infrared spectra of the samples in KBr pellets were recorded on a Specord M-80 spectrophotometer in the range of 1500–300 cm^{-1}.

The EPR measurements were performed with a conventional X-band Brücker ELEXSYS E500 CW-spectrometer operating at 9.5 GHz with 100 kHz magnetic field modulation. Powdered samples of all compounds were into 4 mm diameter quartz tubes. The first derivative of the power absorption spectra have been recorded as a function of the applied magnetic field. Temperature dependence of the EPR spectra in the 3–295 K range was registered using an Oxford Instruments ESP helium-flow cryostat. The temperature dependence analysis of the following spin-Hamiltonian parameters was conducted: the EPR integrated intensity, calculated as a double integral of the EPR signal proportional to the imaginary part of the spin system's complex magnetic susceptibility; the g-factor, reciprocal of the integrated intensity, and the product, $T * I_{int}$, which is proportional to the square of the spin system magnetic moment. The optimization of spin-Hamiltonian parameters and the EPR data simulation were accomplished using the EPR-NMR software package.

Results and discussion

Thermal studies

Thermal behavior of $Gd_2(SO_4)_3 \cdot 8H_2O$ has been studied using simultaneous DTA–TG analysis. Figures 1 and 2 present DTA and TG curves, recorded during heating, in a nitrogen atmosphere, gadolinium sulfate octahydrate, respectively. The equations describing the stages of dehydration and thermal decomposition, onsets of recorded effects associated with these processes (for experiments in air and nitrogen atmosphere) as well as the values of observed and calculated mass losses are given in Table 1. This Table shows also the onsets of effects which are not accompanied by mass change of samples (crystallization, polymorphic transition).

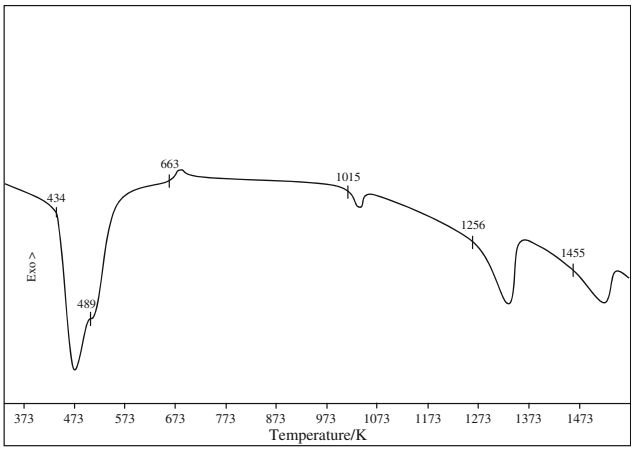

Fig. 1 DTA curve for $Gd_2(SO_4)_3 \cdot 8H_2O$ (a nitrogen atmosphere)

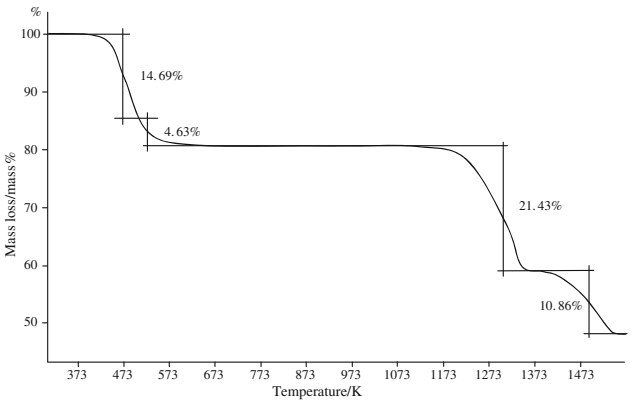

Fig. 2 TG curve for $Gd_2(SO_4)_3 \cdot 8H_2O$ (a nitrogen atmosphere)

The dehydration process of $Gd_2(SO_4)_3 \cdot 8H_2O$ undergoes in two stages. The first endothermic effect with its onset at 434 K (Fig. 1) and with the mass loss (observed—14.69%; calculated—14.35%) corresponds to the loss of six molecules of crystal water. The second stage, starting at 489 K, is associated with loss of two remaining crystal water molecules. The observed mass loss for this stage is 4.63% (the calculated value—4.82%). The exothermic effect, recorded on DTA curve at 663 K, is related to the crystallization of anhydrous and amorphous of $Gd_2(SO_4)_3$. The endothermic effect at 1015 K, also not associated with mass change of samples, corresponds to polymorphic transition of $Gd_2(SO_4)_3$. Thermal decomposition of anhydrous gadolinium sulfate starts at 1256 K. This stage of decomposition is associated with an evolution of gaseous products (sulfur dioxide and oxygen) and a creation of solid $(GdO)_2SO_4$. The observed mass loss for this stage is

Table 1 Thermal analysis data of $Gd_2(SO_4)_3{\cdot}8H_2O$

	Mass loss/%			Onset of recorded effect/K	
	N_2 atmosphere	Air atmosphere	Calculated	N_2 atmosphere	Air atmosphere
$Gd_2(SO_4)_3{\cdot}8H_2O_{(s)} = Gd_2(SO_4)_3{\cdot}2H_2O_{(s)} + 6H_2O_{(g)}$	14.69	14.35	14.47	434 (endo)	437 (endo)
$Gd_2(SO_4)_3{\cdot}2H_2O_{(s)} = Gd_2(SO_4)_{3(s)} + 2H_2O_{(g)}$	4.63	4.80	4.82	489 (endo)	496 (endo)
Crystallization of amorphous $Gd_2(SO_4)_3$				663 (exo)	663 (exo)
Polymorphic transition ($\alpha \rightarrow \beta$)				1015 (endo)	1016 (endo)
$Gd_2(SO_4)_{3(s)} = (GdO)_2SO_{4(s)} + 2\ SO_{2(g)} + O_{2(s)}$	21.43	21.49	21.44	1256 (endo)	1274 (endo)
$2\ (GdO)_2SO_{4(s)} = 2\ Gd_2O_{3(s)} + 2\ SO_{2(g)} + O_{2(g)}$	10.86	10.92	10.72	1455 (endo)	1494 (endo)

21.43% (the calculated value—21.44%). The last endothermic effect, recorded on DTA curve with its onset at 1455 K, is related to the decomposition of $(GdO)_2SO_4$. Solid product of decomposition of gadolinium oxosulfate is Gd_2O_3, gaseous products are sulfur dioxide and oxygen. The observed mass loss for this stage is 10.86% (the calculate value—10.72%). The total mass losses recorded during both measurements in different atmospheres (nitrogen—51.61%, air—51.56%) are in very good agreement with the value calculated (51.45%, Table 1).

XRD studies

The XRD patterns of $Gd_2(SO_4)_3{\cdot}8H_2O$ and all the solid products of dehydration and decomposition were recorded and analyzed. XRD patterns of gadolinium sulfates octahydrate (A) as well as the samples obtained by heating $Gd_2(SO_4)_3{\cdot}8H_2O$ for 12 h at the following temperatures: 453 K (B), 773 K (C), 1073 K (D), 1223 K (E), 1573 K (F) are given in Fig. 3. Powder XRD pattern of $Gd_2(SO_4)_3{\cdot}8H_2O$ revealed that the gadolinium sulfate octahydrate used in the present investigations was monoclinic. The number, positions, and intensities of the diffraction lines recorded on the diffraction pattern of $Gd_2(SO_4)_3{\cdot}8H_2O$ were very similar to the data reported by other authors [10]. The diffraction pattern of sample obtained after heating $Gd_2(SO_4)_3{\cdot}8H_2O$ at 453 K (Fig. 3B) contained the diffraction lines that can be attributed to gadolinium sulfate octahydrate as well as the diffraction lines characteristic for hydrate of gadolinium sulfate with two molecules of crystal water. This fact implies that obtaining pure $Gd_2(SO_4)_3{\cdot}2H_2O$ is very difficult. The structure of this hydrate is unknown so far. The diffraction pattern of the sample (Fig. 3C) obtained by heating $Gd_2(SO_4)_3{\cdot}8H_2O$ at 773 K consisted of peaks due to low-temperature polymorphic modification (α) of anhydrous $Gd_2(SO_4)_3$ [12]. In turn, the powder diffraction pattern of the sample obtained by heating gadolinium sulfate octahydrate at 1073 K (Fig. 3D) consisted of the diffraction lines which positions and intensities were very different in comparison to the other data reported for high-temperature

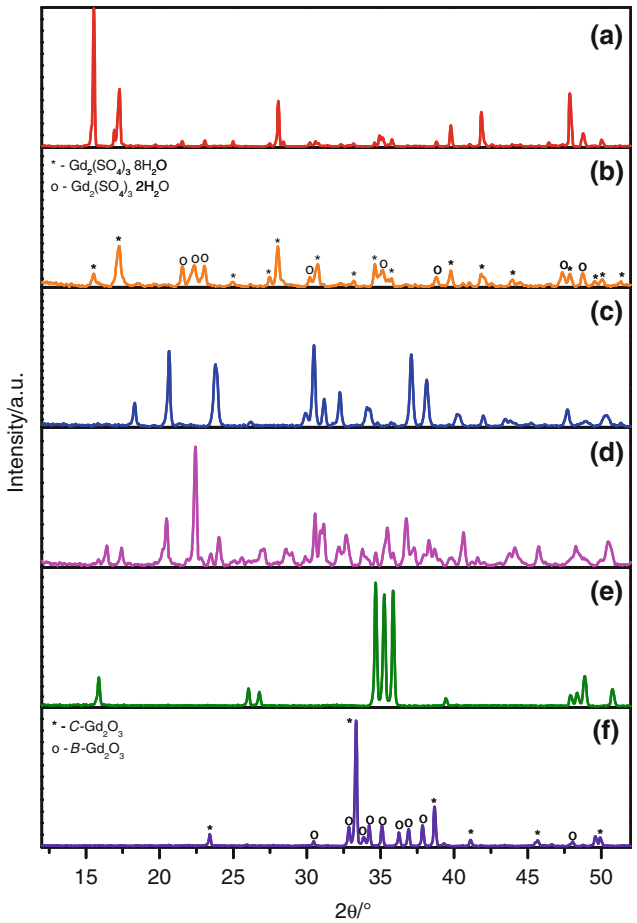

Fig. 3 XRD patterns of: *A* $Gd_2(SO_4)_3{\cdot}8H_2O$; the samples obtained by heating $Gd_2(SO_4)_3{\cdot}8H_2O$ at: *B* 453 K; *C* 773 K; *D* 1073 K; *E* 1223 K; *F* 1573 K

(β) polymorph of $Gd_2(SO_4)_3$ [10, 12]. The interplanar distances (d) and corresponding relative intensities for β-$Gd_2(SO_4)_3$ are summarized in Table 2. XRD measurements of the sample, obtained by heating $Gd_2(SO_4)_3{\cdot}8H_2O$ at 1223 K showed presence of one solid phase, i.e., $(GdO)_2SO_4$ (the diffraction pattern—Fig. 3E). This compound crystallizes in the orthorhombic system with the lattice constants: $a = 0.40553(5)$ nm, $b = 0.41767(6)$ nm, $c = 1.2969(4)$ nm [13]. The XRD pattern of the last

Table 2 Interplanar distances and relative intensities for the diffraction lines characteristic for β-$Gd_2(SO_4)_3$

No.	*d*/nm	I/I_0
1	0.64798	6
2	0.62728	16
3	0.59152	14
4	0.50892	13
5	0.50367	36
6	0.47165	6
7	0.46004	100
8	0.45285	9
9	0.44003	17
10	0.42994	27
11	0.41226	6
12	0.38427	12
13	0.38260	14
14	0.36264	13
15	0.35750	10
16	0.34674	8
17	0.33969	44
18	0.33537	33
19	0.33368	38
20	0.32297	18
21	0.31815	30
22	0.30749	15
23	0.30598	9
24	0.30033	12
25	0.29538	20
26	0.29367	33
27	0.29075	12
28	0.28388	40
29	0.28020	15
30	0.27507	10
31	0.27276	21
32	0.27028	15
33	0.26789	6
34	0.26297	8
35	0.25770	30
36	0.25429	4
37	0.25202	7
38	0.24966	3
39	0.24009	6
40	0.23830	14
41	0.23700	5
42	0.23029	16
43	0.22015	6
44	0.21893	15
45	0.21642	6
46	0.21180	6
47	0.20991	22

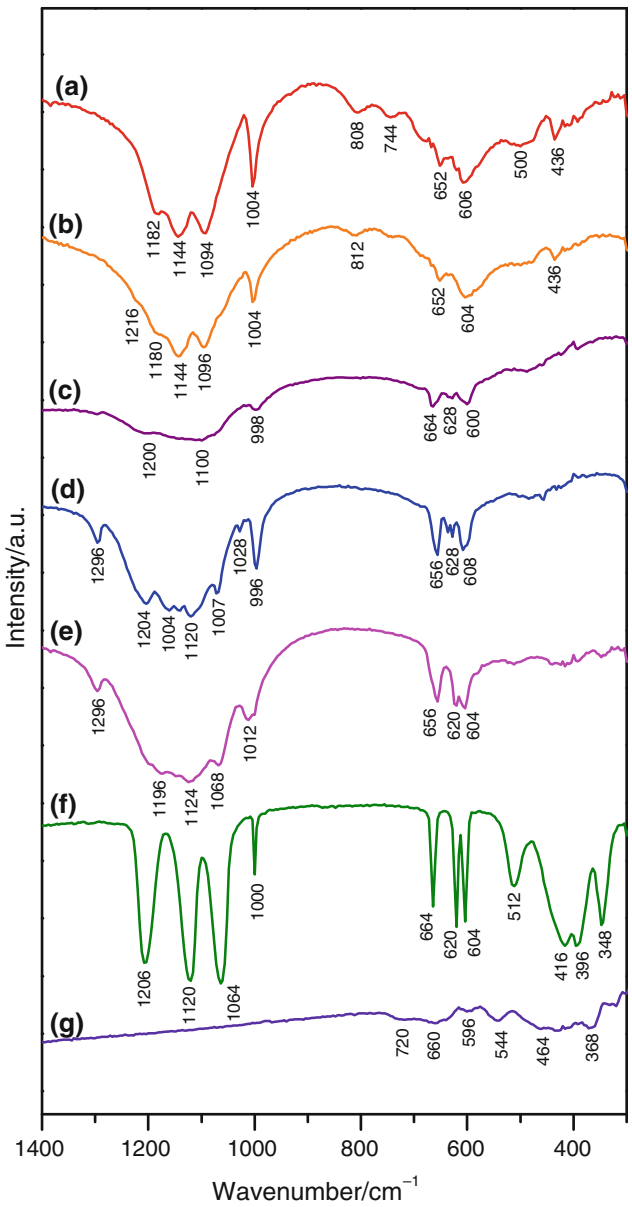

Fig. 4 IR spectra of: *A* $Gd_2(SO_4)_3 \cdot 8H_2O$; the samples obtained by heating $Gd_2(SO_4)_3 \cdot 8H_2O$ at: *B* 453 K; *C* 603 K; *D* 773 K; *E* 1073 K; *F* 1223 K; *G* 1573 K

sample, obtained by heating gadolinium sulfate octahydrate at 1573 K, consisted of peaks due to both polymorphic modification of Gd_2O_3, i.e., *B*-Gd_2O_3 and *C*-Gd_2O_3.

IR spectra

IR spectra of gadolinium sulfate octahydrate (A) as well as the samples obtained by heating $Gd_2(SO_4)_3 \cdot 8H_2O$ for 12 h at the following temperatures: 453 K (B), 603 K (C), 773 K (D), 1073 K (E), 1223 K (F), 1573 K (G) are given in Fig. 4. In the light of literature information [14–16], the broad absorption bands, observed in the IR spectra A–F,

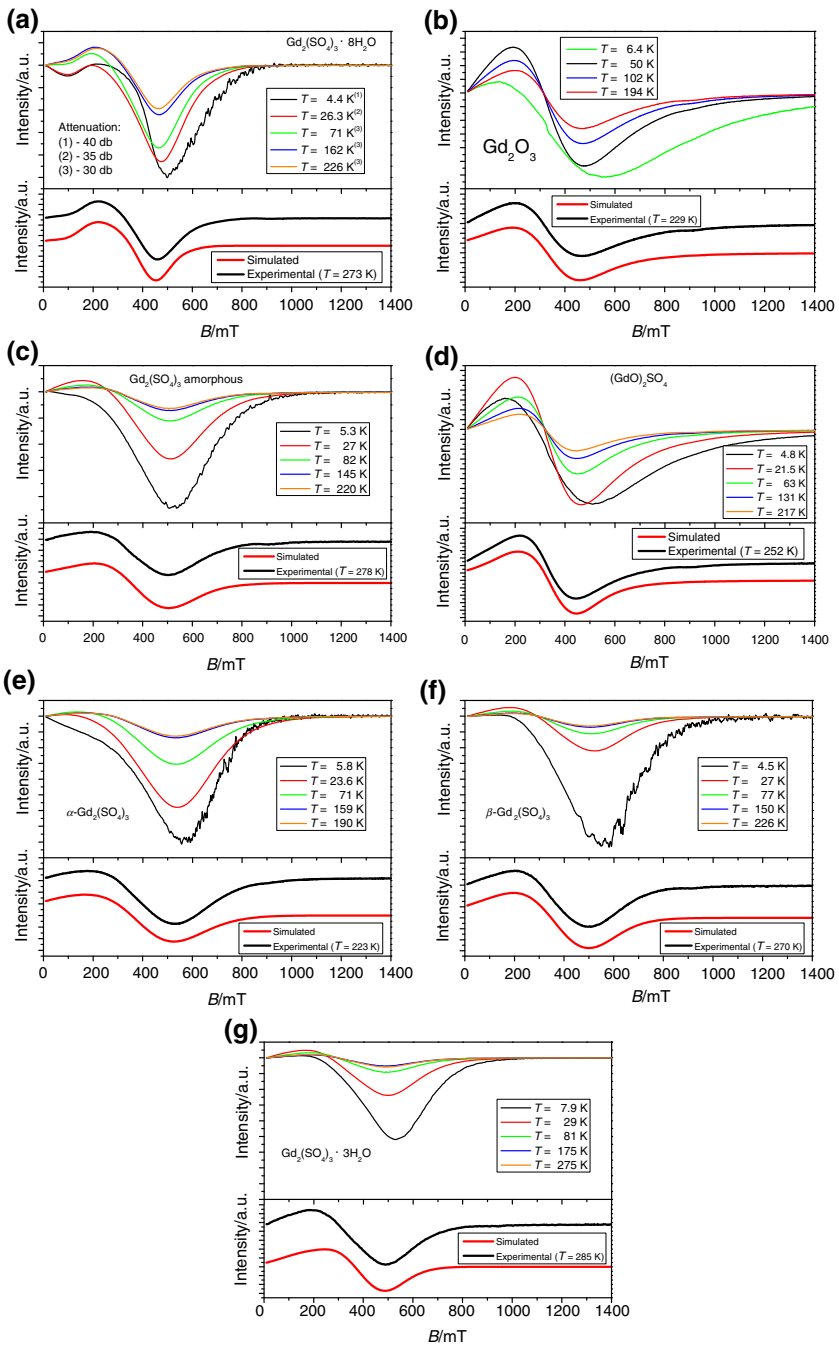

Fig. 5 EPR spectra of the investigated samples:
a $Gd_2(SO_4)_3 \cdot 8H_2O$ (I),
b Gd_2O_3 (II),
c $Gd_2(SO_4)_3$ amorphous (III),
d $(GdO)_2SO_4$ (IV),
e α-$Gd_2(SO_4)_3$ (V),
f β-$Gd_2(SO_4)_3$ (VI),
g $Gd_2(SO_4)_3 \cdot 2H_2O$ (VII)

with their maxima in the range of 1300–1000 cm^{-1}, can be assigned to the stretching modes of S–O bonds in isolated SO_4 tetrahedra. The bands occurring in the wave numbers range of 700–600 cm^{-1} are related to the stretching modes of O–S–O bonds in SO_4 tetrahedra [14–16]. Lack of absorption bands associated with the stretching modes of S–O bonds as well as the stretching vibrations of O–S–O bonds, in the IR spectrum of the sample obtained by heating gadolinium sulfate octahydrate at 1573 K, indicates that thermal decomposition of $Gd_2(SO_4)_3 \cdot 8H_2O$ was complete to gadolinium oxide.

EPR spectra

Figure 5 presents the EPR spectra of the powder gadolinium compounds at selected temperatures. As one can see, the EPR signal (for all compounds) consists of a main asymmetric, broad line with unresolved structure centered about $g \sim 2$. The intensity of the spectrum varies significantly with temperature for all of gadolinium compounds.

Using computer simulation of the experimental EPR spectra we extracted the values of the spin-Hamiltonian parameters required for the determination of structural

Table 3 Parameters of the spin Hamiltonian of the type (1)

	Gd									Gd								
	$\mathbf{g}_x$	$\mathbf{g}_y$	$\mathbf{g}_z$	B_2^0	B_2^2	B_4^0	B_4^2	B_4^4	B_4^{-2}	$\mathbf{g}_x$	$\mathbf{g}_y$	$\mathbf{g}_z$	B_2^0	B_2^2	B_4^0	B_4^2	B_4^4	B_4^{-2}
$Gd_2(SO_4)_3{\cdot}8H_2O$ (I)																		
273 K	1.942	1.941	1.88	300	−22	1.6	1.3	0.6	0	1.942	1.941	1.88	300	97	1.6	1.3	0.6	0
	$\mathbf{J}_x = -40$, $\mathbf{J}_y = 130$, $\mathbf{J}_z = 440$																	
53 K	1.941	1.94	1.89	350	−30	1.8	1.3	0.6	2.5	1.941	1.94	1.89	350	100	1.8	1.3	0.6	2.5
	$\mathbf{J}_x = -66$, $\mathbf{J}_y = 150$, $\mathbf{J}_z = 440$																	
Gd_2O_3 (II)																		
229 K	2.032	2.031	2.034	200	−56	0	0	0	0	2.032	2.031	2.034	200	90	0	0	0	0
	$\mathbf{J}_x = -20$, $\mathbf{J}_y = 10$, $\mathbf{J}_z = 190$																	
$Gd_2(SO_4)_3$ amorphous (III)																		
278 K	1.812	1.815	1.813	325	−100	−4.2	0	0	0	1.812	1.815	1.813	325	140	−4.2	0	0	0
	$\mathbf{J}_x = -20$, $\mathbf{J}_y = 50$, $\mathbf{J}_z = 530$																	
$(GdO)_2SO_4$ (IV)																		
252 K	2.012	2.011	2.015	100	−55	0	0	0	0	2.012	2.011	2.015	100	140	0	0	0	0
	$\mathbf{J}_x = -20$, $\mathbf{J}_y = 50$, $\mathbf{J}_z = 290$																	
α-$Gd_2(SO_4)_3$ (V)																		
223 K	1.811	1.815	1.812	325	−100	−4.8	0	0	0	1.811	1.815	1.812	325	140	−4.8	0	0	0
	$\mathbf{J}_x = -20$, $\mathbf{J}_y = 50$, $\mathbf{J}_z = 290$																	
β-$Gd_2(SO_4)_3$ (VI)																		
270 K	1.861	1.863	1.841	225	−100	−4.8	0	0	0	1.861	1.863	1.841	225	140	−4.8	0	0	0
	$\mathbf{J}_x = -20$, $\mathbf{J}_y = 50$, $\mathbf{J}_z = 620$																	
$Gd_2(SO_4)_3{\cdot}2H_2O$ (VII)																		
285 K	1.832	1.833	1.831	210	−75	0	0	0	0	1.832	1.833	1.831	210	190	0	0	0	0
	$\mathbf{J}_x = -20$, $\mathbf{J}_y = 10$, $\mathbf{J}_z = 670$																	

information concerning these compounds. For Gd^{3+} ions having half-filled f shell with seven electrons and the ground state $^8S_{7/2}$, the spin Hamiltonian should contain spin terms of the type BS (matrix **g**), S_2 (matrix **D**) as well as parameters associated with the high spin terms of the type S_4 and S_6. It is known that a single broad absorption signal encompassing about $g \sim 2$ is assigned to the clusters of Gd^{3+} ions. So additionally, the spin Hamiltonian should have a term of spin–spin interactions (spin A–spin B). The following spin Hamiltonian was used to generate the powder EPR spectra:

$$\mathrm{H_s} = \mu_\mathrm{B} S_i \cdot \mathbf{g}_i \cdot B + S_i \cdot \mathbf{D}_i \cdot S_i + \sum_{m=-l}^{l} B_l^m \cdot O_l^m(S_i) + H_\mathrm{int} \tag{1}$$

where $H_\mathrm{int} = S_\mathrm{A}\mathbf{J}_\mathrm{AB}S_\mathrm{B}$ and i = A, B, $\mathbf{g}_i$ and $\mathbf{D}_i$ are **g** and **D** tensors of the individual center. The first term is the electronic Zeeman term, the second one is the fine structure electronic quadrupole term, and the third one contains S_4 and S_6 terms in Stevens notation, fourth one is the interaction between the two spins, with interaction matrix, **J**. The O_l^m are Stevens operators of degree l, and B_l^m are Stevens parameters. As it is known, the number of B_l^m parameters being different from zero depends on the site symmetry of the paramagnetic center.

Fitting procedure was performed at a fixed temperature (generally being close to room temperature). The temperature and the values of the spin-Hamiltonian parameters calculated for the analyzed gadolinium compounds are collected in Table 3. The presence of three different $\mathbf{g}_i$ components and non-zero values of $B_l^m : B_2^0 B_2^2 B_4^0 B_4^2 B_4^{-2} B_4^4$ in the first compound (I—$Gd_2(SO_4)_3{\cdot}8H_2O$) indicates on a symmetry of the compound being monoclinic type. The gadolinium compounds III, V, and VI have non-zero values of $B_l^m : B_2^0 B_2^2 B_4^0$, the compounds II, IV, and VII have non-zero values of $B_l^m : B_2^0 B_2^2$. Because the interactions between gadolinium ions are enough strong (see **J** values) we could not define parameters of higher order but they still exist. It indicates on a low symmetry of the crystal field at the gadolinium sites in the investigated compounds. For an orthorhombic type symmetry of paramagnetic ion the non-zero values of Stevens parameters are the following $B_l^m : B_2^0 B_2^2 B_4^0$. So, from our investigations it result that the symmetry of Gd^{3+} ions is lower than orthorhombic one for all of the investigated compounds. As one can see from

Table 3, parameters of the spin Hamiltonian, so also local symmetry of gadolinium ions, are the same for amorphous compound (III) and non-hydrated compounds (V, VI) as it could be.

In fitting procedure of EPR lines we have applied two types of lines: Gaussian and Lorentzian-like. The gadolinium compounds I, III, V, VI, and VII are well fitted using prevailing Gaussian line, for the rest of the compounds we applied prevailing Lorentzian-like line. So, the first group of compounds reveals mainly dipole–dipole magnetic interactions, while the second one exchange ones.

Conclusions

Crystals of $Gd_2(SO_4)_3 \cdot 8H_2O$ were obtained by slow crystallization from an aqueous solution. Mechanism of dehydration and decomposition has been established for this salt on the base of TG and XRD investigations. Regardless of a type of used atmosphere for DTA–TG studies, the dehydration of gadolinium sulfate octahydrate and thermal decomposition of anhydrous $Gd_2(SO_4)_3$ undergo in two steps. During heating of anhydrous gadolinium sulfate, the crystallization process and the polymorphic transition were also observed. The new XRD data for high-temperature polymorph of $Gd_2(SO_4)_3$ were given. Thermal decomposition of anhydrous gadolinium sulfate (β-polymorph) to $(GdO)_2SO_4$, and then gadolinium oxysulfate to gadolinium oxide starts, in the air, at temperatures higher than for a nitrogen atmosphere.

From EPR investigations it results that symmetry of gadolinium ions in the investigated compounds is lower than orthorhombic. In some of them prevailing magnetic interactions are of dipole–dipole nature, in others exchange ones.

References

1. Boonchom B. Kinetic and thermodynamic studies of $MgHPO_4 \cdot 3H_2O$ by non-isothermal decomposition data. J Therm Anal Calorim. 2009;98:863–71.
2. Hevroni L, Shamish Z, Danon A. Thermal dehydration and decomposition of copper selenate pentahydrate. J Therm Anal Calorim. 2009;98:367–70.
3. Rao RP. Preparation and characterization of fine-grain yttrium-based phosphors by sol-gel process. J Electrochem Soc. 1996; 143:189–97.
4. Erdei S, Roy R, Harshe G, Juwhari H, Agrawal D, Ainger FW, et al. The effect of powder preparation processes on the luminescent properties of yttrium oxide based phosphor materials. Mater Res Bull. 1995;30:745–53.
5. Rane KS, Uskaikar H, Pednekar R, Mhalsikar R. The low temperature synthesis of metal oxides by novel hydrazine method. J Therm Anal Calorim. 2007;90:627–38.
6. Šulcova P, Trojan M. Thermal synthesis of the $(Bi_2O_3)_{1-x}(Er_2O_3)_x$ pigments. J Therm Anal Calorim. 2007;88:111–3.
7. Šulcova P, Trojan M. Thermal analysis of pigments based on Bi_2O_3. J Therm Anal Calorim. 2006;84:737–40.
8. Nahdi K, Férid M, Ayadi MT. Thermal dehydration of $CeP_3O_9 \cdot 3H_2O$ by controlled rate thermal analysis. J Therm Anal Calorim. 2009;96:455–61.
9. Basavaraja S, Venkatataraman A, Ray A. Interpretation of partial thermal decomposition mechanism of $Dy_2(SO_4)_3 \cdot 8H_2O$. Thermal, electrical and spectroscopic techniques. J Therm Anal Calorim. 2009;96:419–25.
10. Hummel HU, Fischer E, Fischer T, Joerg P, Pezzei G. Structure and thermal manner of gadolinium sulfate octahydrate $Gd_2(SO_4)_3 \cdot 8H_2O$. Z Anorg Allg Chem. 1993;619:805–10. (in German).
11. Bayer E, Leppert J, Grabmaier BC, Blasse G. Time-resolved spectroscopy and energy transfer in Pr^{3+}-doped $Gd_2(SO_4)_3 \cdot 8H_2O$. Appl Phys A. 1995;61:177–81.
12. Sato A. Formation of amosphous lanthanide sulfates and their crystallization. Thermochim Acta. 1988;124:217–28.
13. Tomaszewicz E. Studies on the reactivity in the solid state between some rare-earth metal oxides Ln_2O_3 where Ln = Y, La, Nd, Sm, Eu, Gd, Dy, Ho, Er, Lu and metal sulfates(VI) MSO_4 where M = Ni, Cu, Zn, Cd. J Mater Sci. 2006;41:1675–80.
14. Baran EJ, Aymonino PJ. The IR spectra of silver and thalium(I) sulphates. Spectrochim Acta. 1968;24A:288–91.
15. Dawson P, Hargreave MM, Wikinson GR. Polarized IR reflection, absorption and laser Raman studies on a single crystal of $BaSO_4$. Spectrochim Acta. 1977;33A:83–93.
16. Durie RA, Milne JW. Infrared spectra of anhydrous alkali metal sulphates. Spectrochim Acta. 1978;34A:215–20.